Supporting Information

Single Nanosheet Can Sustainably Generate Oxygen and Inhibit Respiration Simultaneously in Cancer Cell

Wei-Qiang Huang,[ab] Fei Wang,[c] Ai-Zong Shen,*[d] Lei Zhang,[d] Xuan Nie,[b] Ze Zhang,*[b] Guang Chen,[b] Lei Xia,[b] Long-Hai Wang,[b] Sheng-Gang Ding,*[e] Qing-Yong Meng,[f] Wen-Jian Zhang,[b] Chun-Yan Hong*[b] and Ye-Zi You*[ab]

a. The Department of Pharmacy, The First Affiliated Hospital of USTC, Division of Life Sciences and Medicine , University of Science and Technology of China, Hefei, Anhui, 230026, China

b. Hefei National Laboratory for Physical Sciences at the Microscale, Hefei, Anhui 230026, China

c. Neurosurgical Department，The First Affiliated Hospital of USTC, Division of Life Sciences and Medicine, Hefei, Anhui, 230026, China

d. The Department of Pharmacy, The First Affiliated Hospital of USTC, Division of Life Sciences and Medicine, Hefei, Anhui, 230026, China

e. Anhui Medical University, Affiliated Hospital, Department of Pediatric, Hefei, Anhui, 230026, China

f. Anhui Medical University, Affiliated Hospital, Department of Radiotherapy, Anhui, Peoples R China.

Methods and materials

Materials: Ti_2AlC (99%, Bike), HF solution (40%, Aladdin), NaOH (Aladdin), Chlorin e6 (Aladdin), TiO (Aladdin), (2-aminoethyl) phosphonic acid (Aladdin), dimethyl sulfoxide (99%, Aladdin), 3,3'5,5'-tetramethyl benzidine (Aladdin), DMEM medium (Hyclone), 1,4-dicarboxybenzene (Aladdin), enhanced ATP assay kit (Beyotime), pimonidazole HCl (MCE), 1,3-diphenylisobenzofuran (Aladdin), 1-(3-dimethylaminopropyl)-3-ethylcarbodiimide hydrochloride (Aladdin), 2',7'-dichlorofluorescein diacetate (Beyotime), N-hydroxysuccinimide (Aladdin), antipimonidazole antibody (Hypoxyprobe, Inc), FBS (Sigma) were used as received.

Synthesis of Ti_2C nanosheets: First, Ti_2AlC were first immersed in 30% HF solution. Then, the suspension was stirred at a speed of 700 rpm for 48 h at 50 ^oC. The HF solution was decanted and the solids were collected. Distilled water was used to wash the solids twice. Finally, the obtained solids were dried in Ar_2/H_2 atmosphere.[1]

Surface group modification: First, Ti_2C flakes were dispersed in NaOH solution. The mixture was stirred for 12h at room temperature. Then, NaOH solution was decanted and the solids were washed twice by distilled water. Finally, the solids were dried.[1b, 2]

$Ti_2C(OH)_2$ (50.0 mg) was added into 20.0 ml water, and then the solution was sonicated in ice water with a probe sonication for 3.0 h (Amplifier: 60%, On/Off cycle: 1 s/4 s). The large-sized $Ti_2C(OH)_2$ and Ti_2AlC were removed by centrifugation.

Synthesis of $Ti_2C(OH)_2$-Ce6 nanoparticles: EDC (24.0 mg), NHS (48.0 mg), and Ce6 (2.0 mg) were mixed and stirred in 4 mL DMSO solution for 3 h, then 8.0 mg $Ti_2C(OH)_2$ and 0.35 mg (2-aminoethyl) phosphonic acid dispersed in 1.0 mL water were added into DMSO solution[3]. After 24 h, unreacted

Ce6 were removed through centrifugation, $Ti_2C(OH)_2$-Ce6 were washed twice with distilled water. The loading efficiency of $Ti_2C(OH)_2$-Ce6 is 0.19g per gram calculated as below.

$$\frac{m_{Ti}}{m_{Ti2C(OH)2}} = 68.8\%$$

$$\frac{M_P}{M_{(2-aminoethyl)\ phosphonic\ acid}} = 0.2479$$

$$\frac{m_P}{m_{Ti}} = 0.0145 \quad \text{via ICP-MS}$$

The amount of Ce6 added into the reaction was much higher than (2-aminoethyl) phosphonic acid, thus we could consider that the mole ratio of (2-aminoethyl) phosphonic acid to Ce6 is 1:1.

$$\frac{m_{Ce6}}{m_{Ti2C(OH)2}} = \frac{n_{Ce6} * M_{Ce6}}{\frac{m_{Ti}}{68.8\%}}$$

$$n_{Ce6} = \frac{m_{(2-aminoethyl)\ phosphonic\ acid}}{M_{(2-aminoethyl)\ phosphonic\ acid}} = \frac{m_P}{M_P}$$

$$m_{Ti} = \frac{m_P}{0.0145}$$

$$\frac{m_{Ce6}}{m_{Ti2C(OH)2}} = \frac{M_{Ce6} * 0.0145 * 68.8\%}{M_P} = 0.192$$

Catalytic activity detection of $Ti_2C(OH)_2$: O_2 concentration in solution was detected by an oxygen probe JPB-70A, catalytic activity of $Ti_2C(OH)_2$ was detected by O_2 concentration dispersed in solution. 50 mM H_2O_2 and 0.5 mg/mL catalyst were prepared to detect continuous O_2 production. In order to quantitatively evaluate the catalytic efficiency, the remaining amount of H_2O_2 in solutions was detected by $Ti(SO_4)_2$.

Single oxygen detection: 1,3-Diphenylisobenzofuran (DPBF) in ethanol (20.0 μg/mL) was mixed with $Ti_2C(OH)_2$-Ce6 in the presence or absence of H_2O_2 (30.0 mM). The UV/Vis spectra of DPBF was recorded every 30 seconds under 660 nm laser irradiation (0.15 W/cm^2).

Cytotoxicity assay: 4T1 cell were first planted in 96 plants for 24.0 h for MTT assay. $Ti_2C(OH)_2$-Ce6 and Ce6 were added into plates. After 4 h, the medium was discarded, and 4T1 cells were washed by PBS twice. Then 4T1 cells were incubated under N_2 or air atmosphere for 30 min, then received 5 min 660 nm laser irradiation. After another 12.0 h incubation, cell viability was determined by standard MTT method.

In vitro photothermal and photodynamic ablation: 4T1 cells were first seeded in 96-well plates, and then incubated for 24.0 h. The culture medium was removed, and $Ti_2C(OH)_2$-Ce6 dispersed in10% FBS DMEM was added into wells (100 μL) and incubated for 4.0 h. Then 808 nm (0.8 W/cm^2) or 660 nm (0.15 W/cm^2) were used to irradiate each well. After another 12.0 h, cell viability was determined by standard MTT method.

Mitochondrial Bioenergetics: The impact of $Ti_2C(OH)_2$ on mitochondrial bioenergetics was investigated by Seahorse Extracellular Flux analyser. HeLa cells (1x10^5) were first planted in 96-well plates, followed by culturing at 37 ^{o}C for 12.0 h. $Ti_2C(OH)_2$-Ce6 (75.0 μg/mL) were suspended in growth medium and incubated for 24.0 h. Then, the medium was removed, and the cell were washed twice by XF assay medium (Seahorse). Finally, XF assay medium was added into each wells, and cells were incubated at 37 ^{o}C in a CO_2-free incubator for 1.0 h. OCR was measured by Seahorse XF96 extracellular flux analyser.

ATP production measurement: HeLa cells were seeded in 24-well plates at 2×10^5 cells/well in 10% FBS DMEM medium, then 75.0 μg/mL $Ti_2C(OH)_2$-Ce6 were suspended in growth medium and incubated for 24.0 h. The ATP level in cells was measured using enhanced ATP assay kit which operated on ice. The luminescence intensity was measured by microplate reader.

Absorbed protein analysis: $Ti_2C(OH)_2$ were first incubated with HeLa cells for about 12.0 h, wash the cell twice with PBS, then cells were lysed. The $Ti_2C(OH)_2$ which entered cells were collected through centrifugation. Then the protein which absorbed on the surface of $Ti_2C(OH)_2$ were analyzed by company APPLIED PROTEIN TECHNOLOGY.

In vivo phototoxicity therapy and systemic toxicity in vivo: Female Bulb/c mice (5 weeks) were purchased from Beijing Vital River Laboratory Animal Technology Co., Ltd, the Administrative Committee on Animal Research in University of Science and Technology of China approved the protocols for all animal assays in this paper. About 100 μL 4T1 cells in PBS (about 1×10^6 cells per mouse) were implanted subcutaneously into mice. After we transplanted the 4T1 cells into mice, we observed the tumor growth at frequent intervals. The tumor volume was calculated: $V(mm^2)=1/2\times length\times width^2$. When the tumor volume reached 200 mm^2, the mice were randomly divided into 7 groups (n=5, each group):

(Group 1) PBS administration.

(Group 2) only laser irradiation (808 nm, 1.0 $W\bullet cm^{-2}$, 5 min and 660 nm, 0.25 $W\bullet cm^{-2}$, 5 min).

(Group 3) only $Ti_2C(OH)_2$-Ce6 (5 $mg\bullet kg^{-1}$).

(Group 4) $Ti_2C(OH)_2$-Ce6 (5 $mg\bullet kg^{-1}$) combined with laser irradiation (808 nm, 1.0 $W\bullet cm^{-2}$, 5 min).

(Group 5) $Ti_2C(OH)_2$-Ce6 (5 $mg\bullet kg^{-1}$) combined with laser irradiation (660 nm, 0.25 $W\bullet cm^{-2}$, 5 min).

(Group 6) $Ti_2C(OH)_2$-Ce6 (5 mg•kg^{-1}) combined with laser irradiation (808 nm, 1 W•cm^{-2}, 5 min and 660 nm, 1 W•cm^{-2}, 5 min).

(Group 7) Ce6 (1 mg•kg^{-1}) combined with laser irradiation (660 nm, 0.25 W•cm^{-2}, 5 min).

The body weight and tumor size of each mouse was recorded every day. After two weeks treatment, mice were humanly killed and then all heart, liver, spleen, lung, kidney and tumor were collected fast. In order to observe systemic toxicity, all organs were fixed for H&E staining.

Tissue hypoxia immunofluorescence assay: The hypoxia marker pimonidazole HCl were used as hypoxia probe. First, 4T1 tumor-bearing mice were intravenously injected with PBS or $Ti_2C(OH)_2$-Ce6. After 24.0 h, pimonidazole HCl (60 mg/kg) were intraperitoneal injected, then mice were killed humanly and tumor tissues were harvested about 90 min after injection. Frozen sections of the tumor were taken at optimal cutting temperature. Tumor sections were then incubated with antipimonidazole antibody (FITC-MBb1). Nuclei were stained with DAPI and images were obtained by confocal microscopy. The hypoxia positive area was analyzed by Image-J.

In vivo imaging and biodistribution analysis: Three 4T1 tumor-bearing mice were intravenously injected with $Ti_2C(OH)_2$-Ce6 and free Ce6 respectively. After 24.0 h, mice were killed humanly, then heart, liver, kidney, spleen, lung and tumor were collected quickly. The fluorescence intensity in all organs were analyzed through in-Vivo Imaging system IVIS spectrum.

Statistics: Triplicate data were analyzed with Student's t-test using omicshare tools; the significance level was set at $p < 0.05$. Significant statistical differences are indicated by asterisks in corresponding figures.

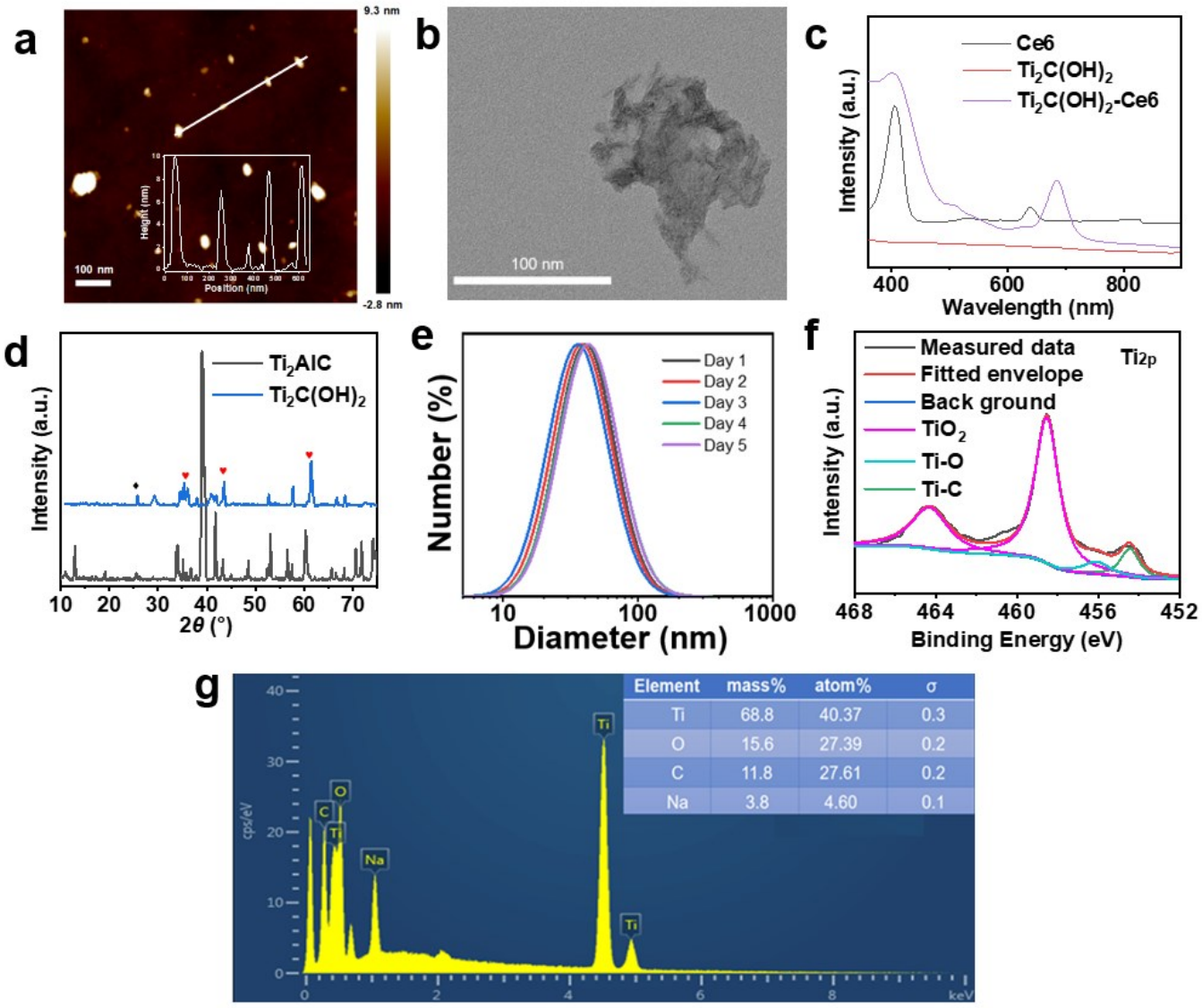

Figure S1. (a) AFM images of $Ti_2C(OH)_2$–Ce6 and AFM measured thickness of $Ti_2C(OH)_2$–Ce6. (b) TEM images of $Ti_2C(OH)_2$–Ce6. (c) UV/Vis spectrum of Ce6, $Ti_2C(OH)_2$ and $Ti_2C(OH)_2$–Ce6. (d) XRD spectra of $Ti_2C(OH)_2$. (e) DLS measured data of $Ti_2C(OH)_2$ incubated in 10% FBS medium from day 1 to day 5. (f) XPS spectra of TiO. (g) EDS spectra of $Ti_2C(OH)_2$.

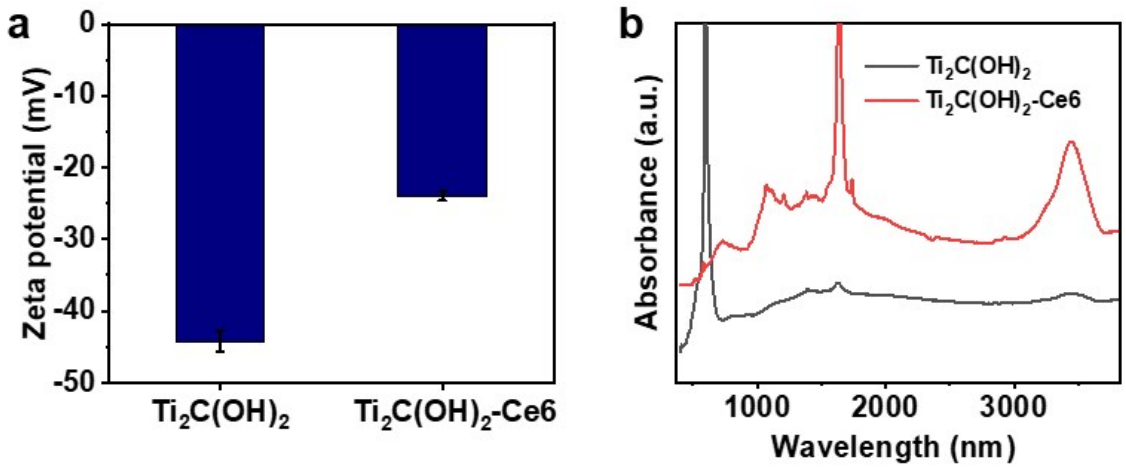

Figure S2. (a) Zeta potential of $Ti_2C(OH)_2$ and $Ti_2C(OH)_2$-Ce6. (b) FT-IR spectra of $Ti_2C(OH)_2$ and $Ti_2C(OH)_2$-Ce6.

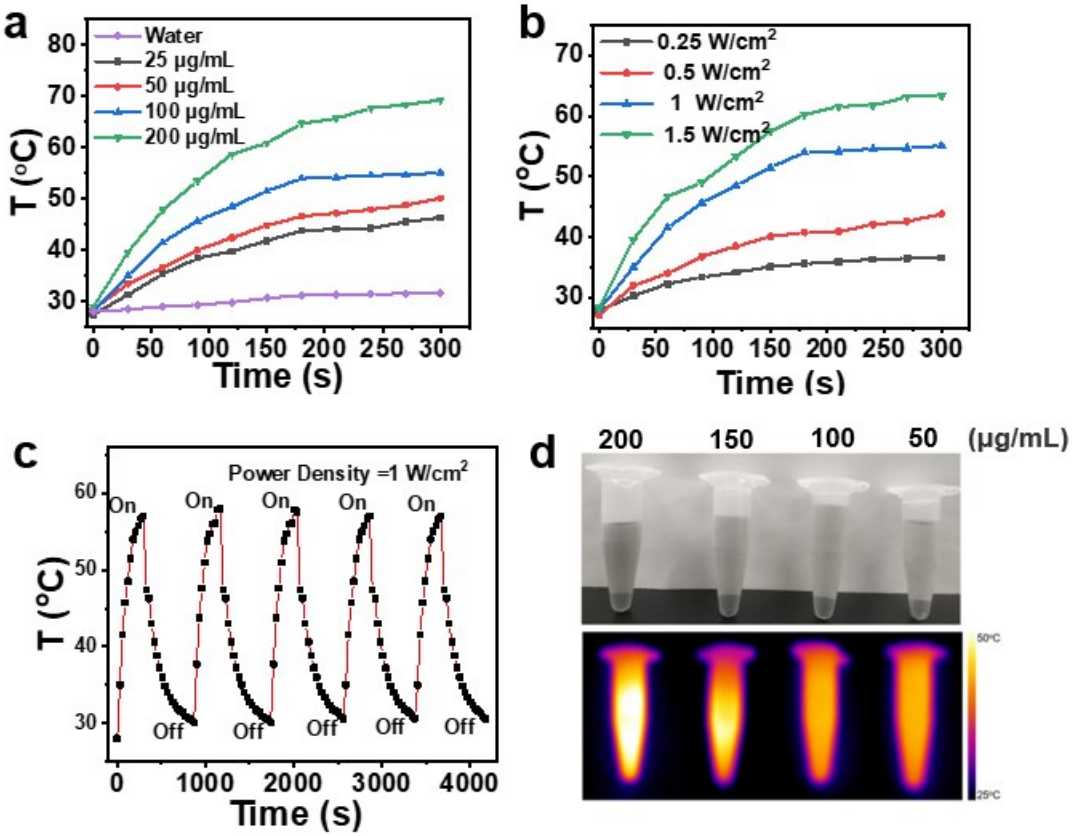

Figure S3. Photothermal properties of $Ti_2C(OH)_2$: (a) Temperature curves of $Ti_2C(OH)_2$ in water solutions at different concentrations. (b)Temperature curves of 100μg/mL $Ti_2C(OH)_2$ in water solutions at different power densities. (c) Photothermal stability of $Ti_2C(OH)_2$ (100 μg/ml). Heating of a suspension of the $Ti_2C(OH)_2$ in water for five laser on/off cycles with an 808 nm NIR laser at power density of 1.0 W/cm^2. (d) Optical photographs and thermal images of $Ti_2C(OH)_2$ in water solutions after laser irradiation.

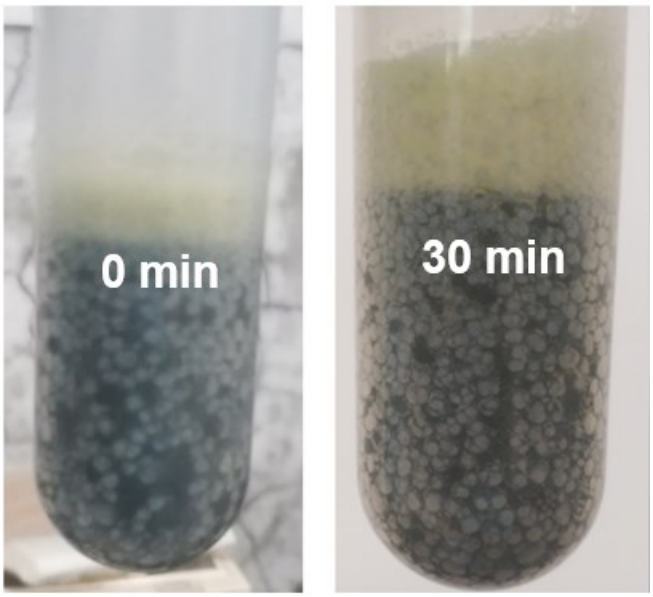

Figure S4. The morphology of $Ti_2(OH)_2$ added in H_2O_2 solution.

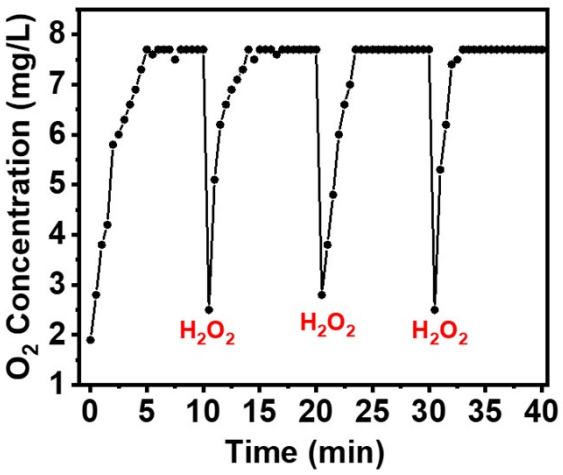

Figure S5. O_2 generation by change the H_2O_2 for 4 cycles in the $Ti_2C(OH)_2$ solution.

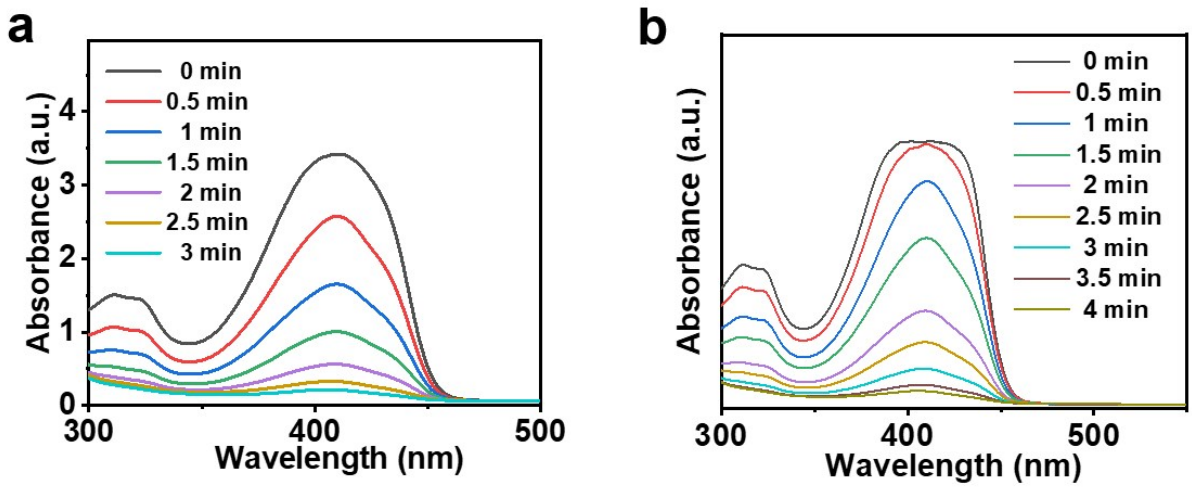

Figure S6. Decay curves of DPBF absorption in $Ti_2C(OH)_2$-Ce6 with (a) or without H_2O_2 solution (b) after different irradiation time.

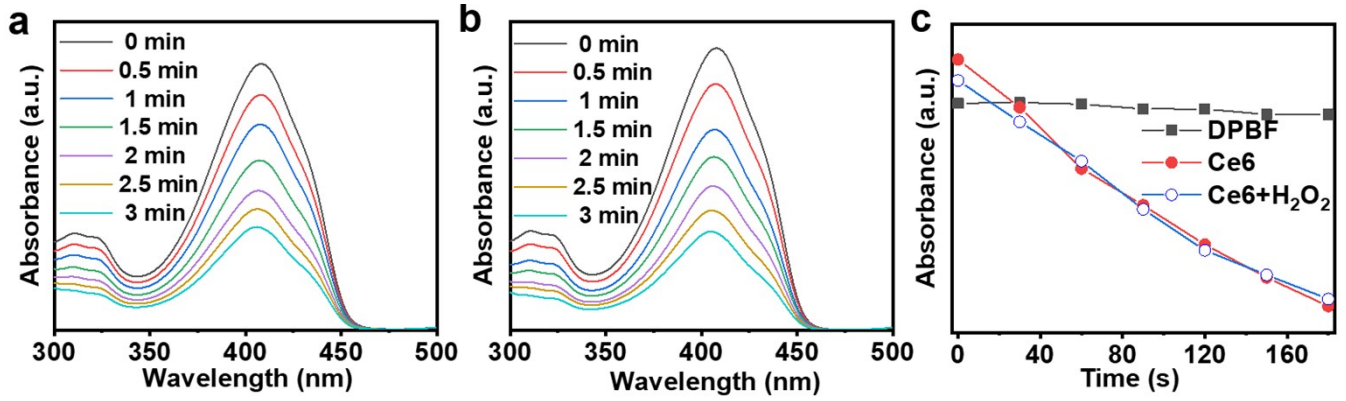

Figure S7. Decay curves of DPBF absorption in Ce6 with (a) or without H_2O_2 solution (b) after different irradiation time. (c) Decay curves of DPBF absorption at 410 nm in Ce6 solution with or without H_2O_2 after different time of irradiation.

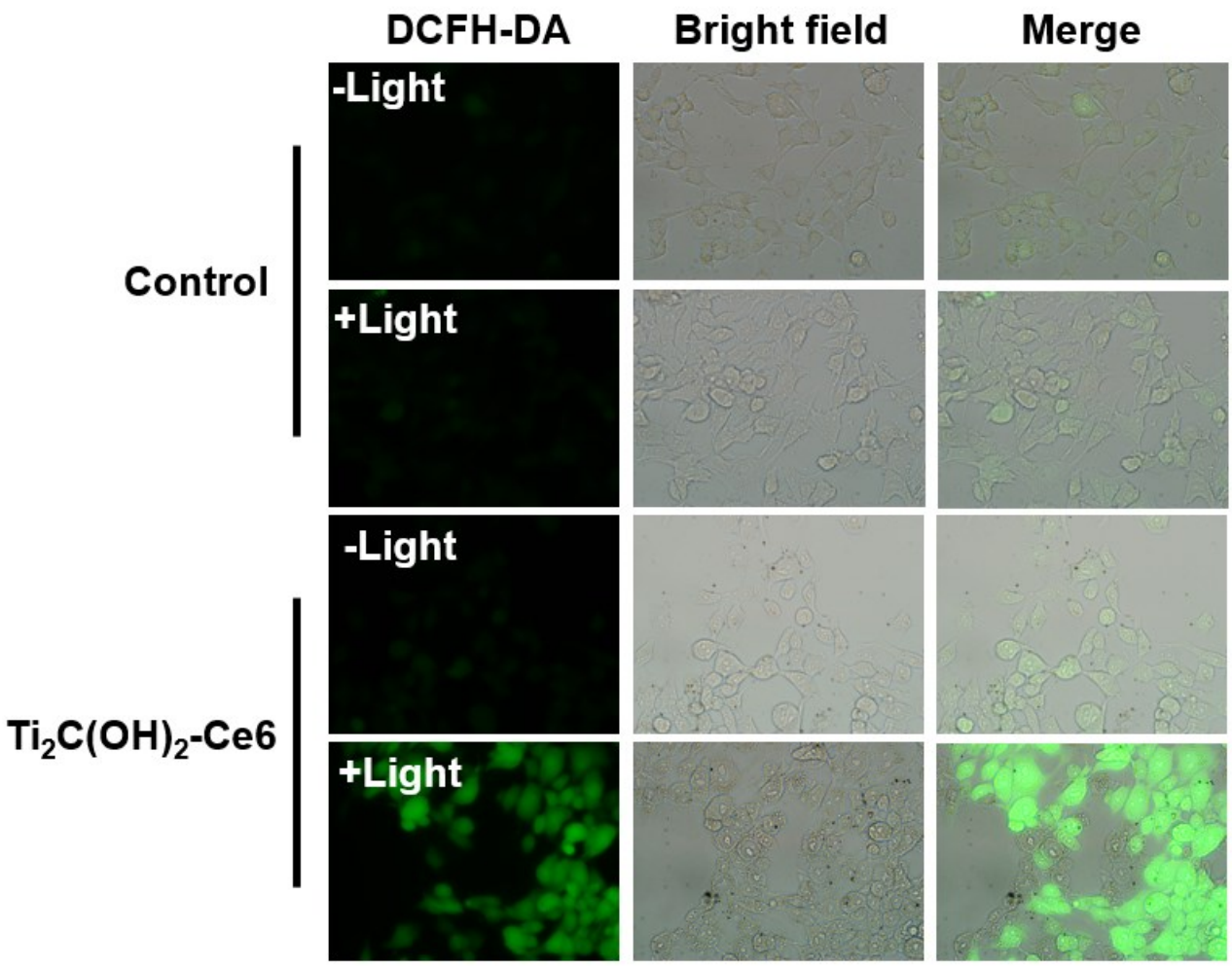

Figure S8. 4T1 cells incubated with $Ti_2C(OH)_2$-Ce6 with irradiation, green fluorescence represents intracellular ROS level.

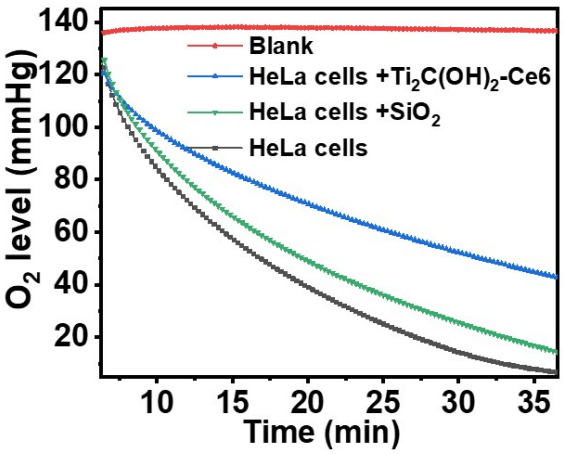

Figure S9. O_2 consumption level of HeLa cells after incubation with $Ti_2C(OH)_2$-Ce6 or SiO_2.

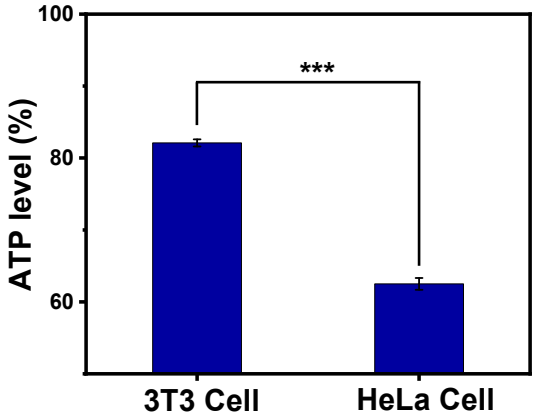

Figure S10. ATP levels in 3T3 cells and HeLa cells after incubated with $Ti_2C(OH)_2$.

Mitochondrial heat shock 60kD protein 1 variant 1
Stomatin-like protein 2, mitochondrial
Prelamin-A/C
NADH dehydrogenase [ubiquinone] 1 beta subcomplex subunit 2, mitochondrial
Cytochrome b5 type B
ATP synthase subunit alpha, mitochondrial
Carbamoyl-phosphate synthase [ammonia], mitochondrial
Lon protease homolog, mitochondrial
ATP synthase F(0) complex subunit C3, mitochondrial
10 kDa heat shock protein, mitochondrial
Hsp90 co-chaperone Cdc37
Protein MTO1 homolog, mitochondrial
ATP synthase subunit beta, mitochondrial
Heat shock protein HSP 90-alpha

Figure S11. Fourteen types of proteins absorbed on the nanosheets related to mitochondria respiration.

ATP synthase F(0) complex subunit C3, mitochondrial

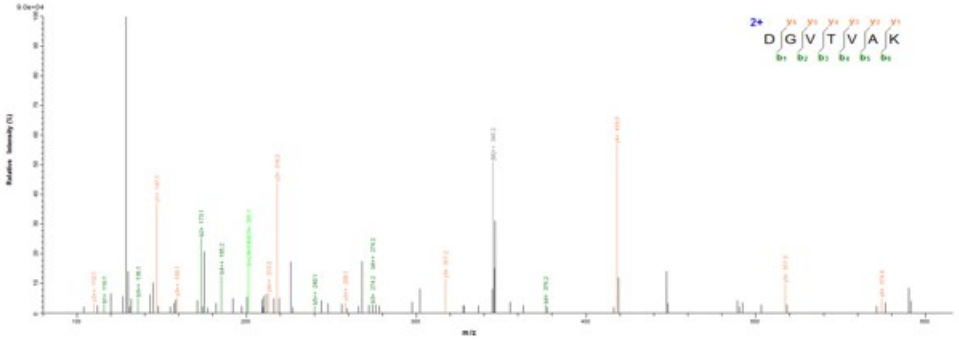

ATP synthase subunit alpha, mitochondrial

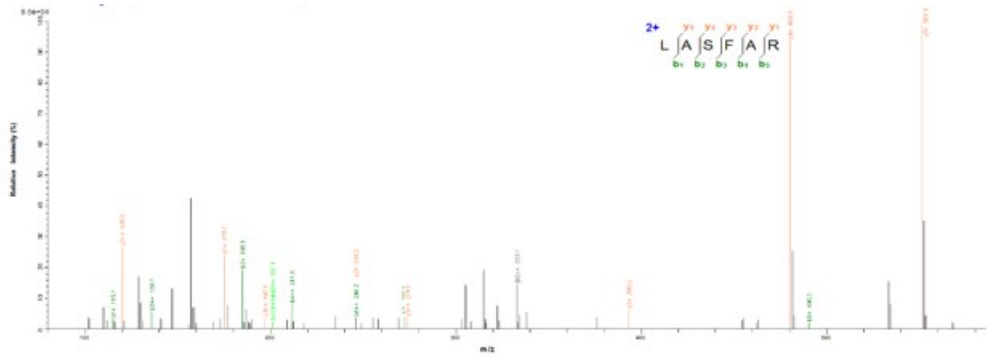

NADH dehydrogenase [ubiquinone] 1 beta subcomplex subunit 2, mitochondrial

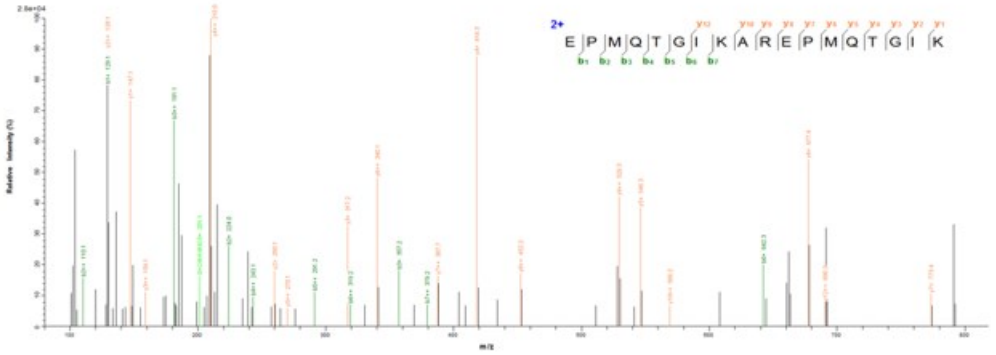

Figure S12. MS spectra of peptides belong to proteins which connected with mitochondria respiration.

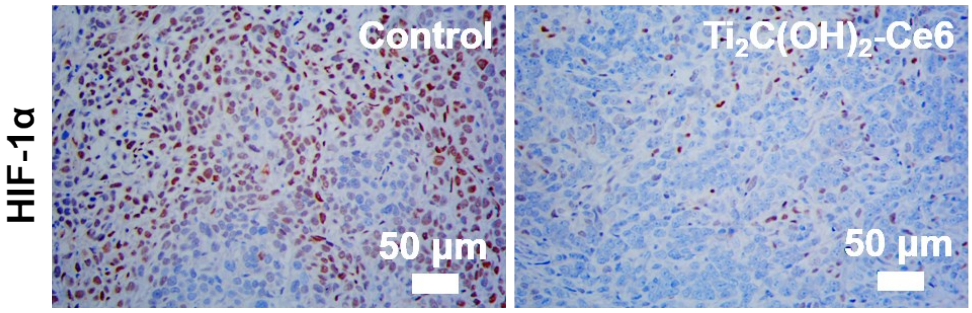

Figure S13. Immunohistochemical analysis of 4T1 tumor slices collected from untreated control mice and the mouse injected with $Ti_2C(OH)_2$-Ce6.

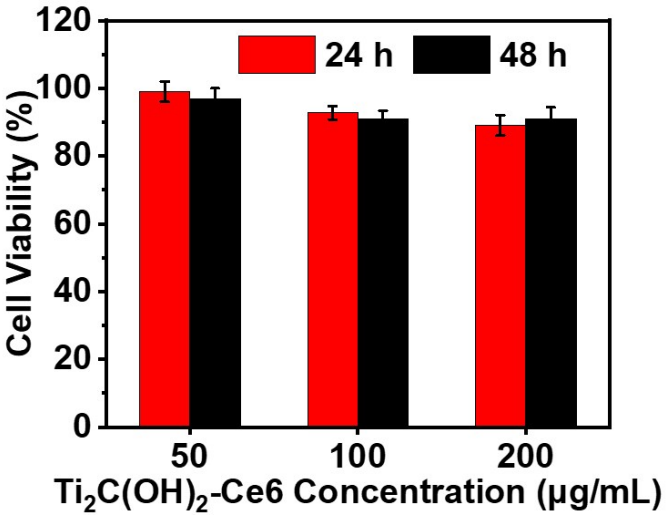

Figure S14. The toxicity of $Ti_2C(OH)_2$-Ce6 after 24h and 48 h incubation in HeLa cells.

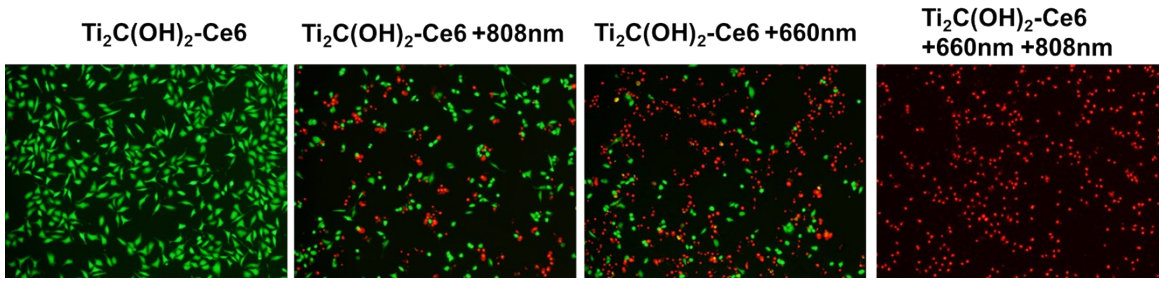

Figure S15. The PDT and PTT efficiency in vitro, the live/dead staining.

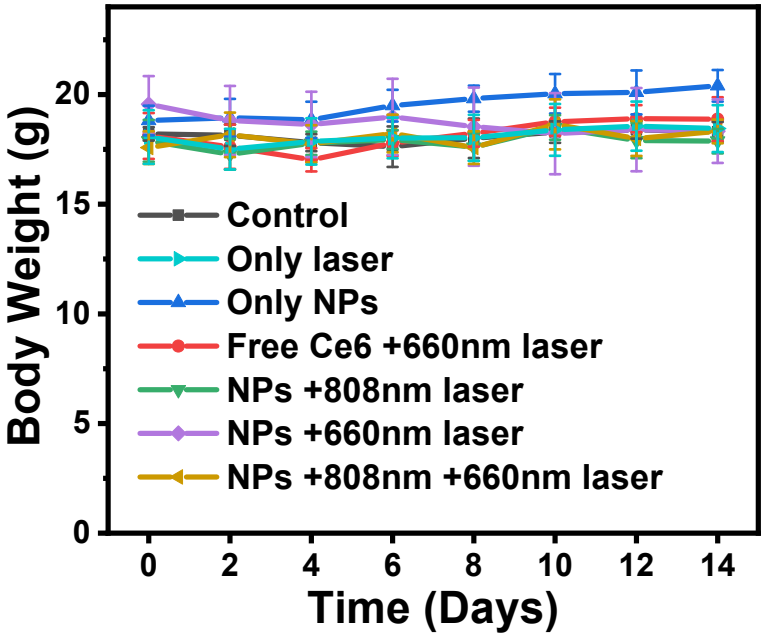

Figure S16. The changes of body weight for different groups. NPs represent $Ti_2C(OH)_2$–Ce6.

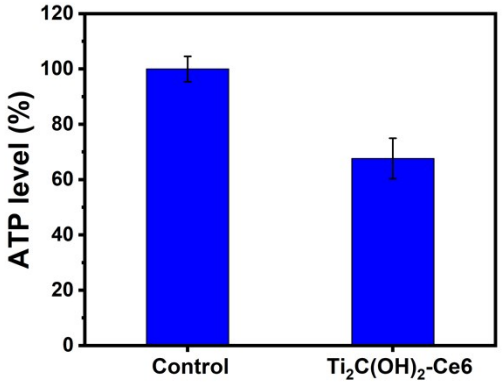

Figure S17. ATP levels in tumor sites treated with or without $Ti_2C(OH)_2$-Ce6.

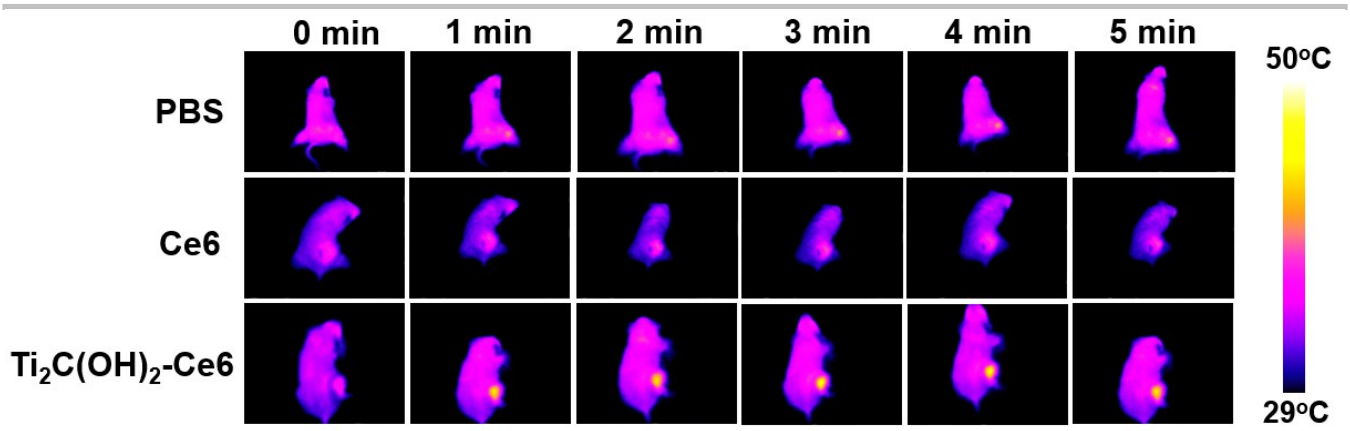

Figure S18. Thermal images of mice treated with PBS, Ce6 and $Ti_2C(OH)_2$-Ce6 under 808 nm laser irradiation at different times.

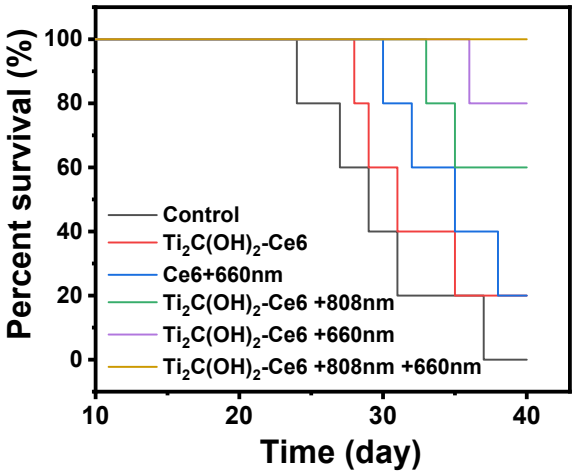

Figure S19. The mouse survival data.

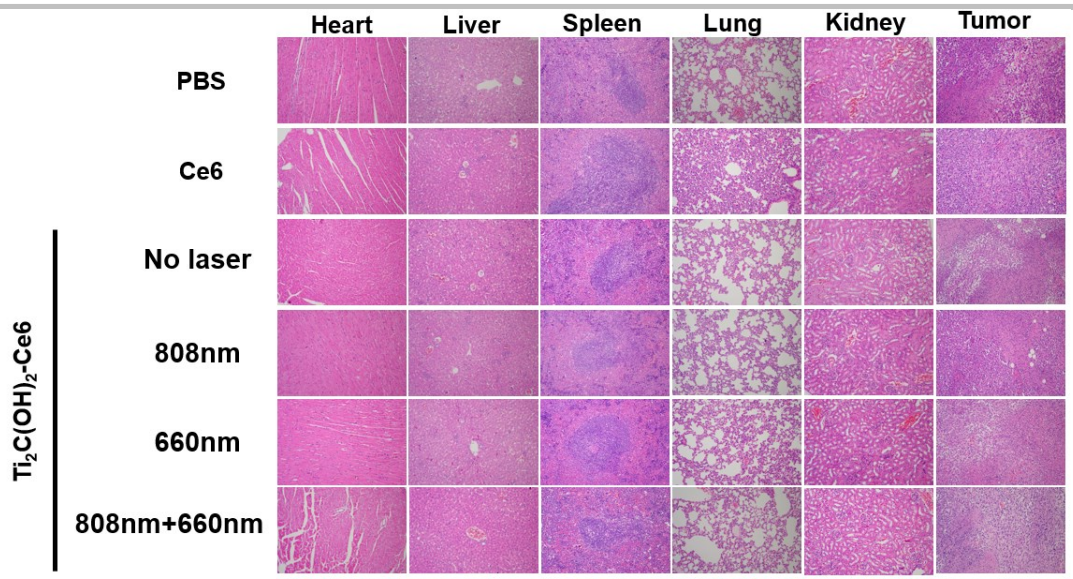

Figure S20. H&E stained histological images of tissue sections from major organs after 14 d of different treatment. PBS was used as a control.

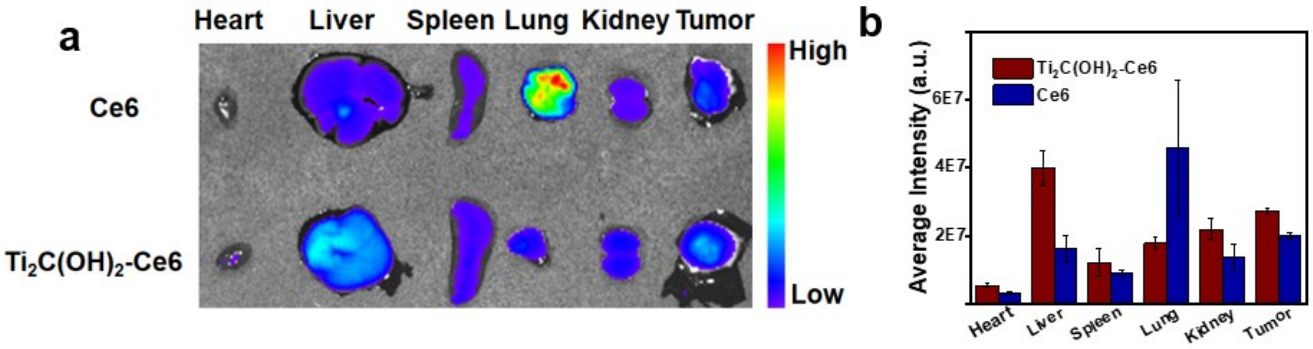

Figure S21. (a) Bio-imaging of major organs and tumor after injection at 24 h. (b) Semi-quantitative biodistribution in mice by measuring average fluorescence intensity in major organs and tumor.

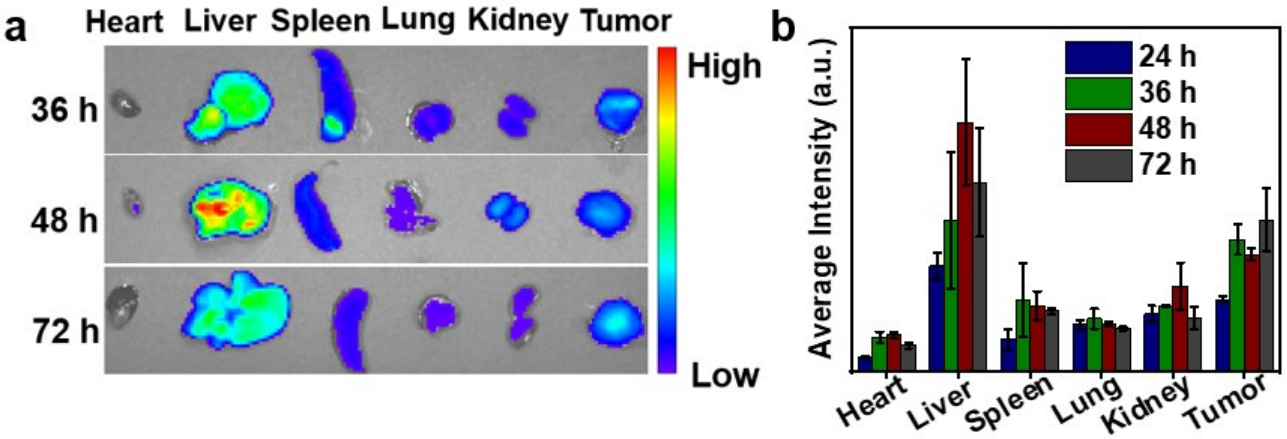

Figure S22. (a) Bio-imaging of major organs and tumor after injection of $Ti_2C(OH)_2$-Ce6 at 36 h, 48 h and 72 h. (b) Semi-quantitative biodistribution in mice by measuring average fluorescence intensity in major organs and tumor.

Supplementary References

1. a) S. Lai, J. Jeon, S. K. Jang, J. Xu, Y. J. Choi, J. H. Park, E. Hwang, S. Lee, *Nanoscale* 2015, **7**, 19390-19396; b) J. Li, X. Yuan, C. Lin, Y. Yang, L. Xu, X. Du, J. Xie, J. Lin, J. Sun, *Adv. Energy Mate.,* 2017, **7**, 1602725; c) H. Xu, X. Yin, X. Li, M. Li, L. Zhang, L. Cheng, *Funct. Compos. Struct.,* 2019, **1**, 015002.
2. S. Shen, T. Ke, K. Rajavel, K. Yang, D. Lin, *Small,* 2020, e2002433.
3. X. Y. Yang, D. Y. Wang, J. W. Zhu, L. Xue, C. J. Ou, W. J. Wang, M. Lu, X. J. Song, X. C. Dong, *Chem. Sci.,* 2019, **10**, 3779-3785.